



ELSEVIER

Journal of Chromatography A, 728 (1996) 33–45

JOURNAL OF  
CHROMATOGRAPHY A

## Study of the flow development during the slurry packing of microcolumns for liquid chromatography

Tatiana Zimina<sup>a,\*</sup>, Roger M. Smith<sup>a</sup>, Julian C. Highfield<sup>b</sup>, Peter Myers<sup>c</sup>, Brian W. King<sup>c</sup>

<sup>a</sup> Department of Chemistry, Loughborough University of Technology, Loughborough, Leics. LE11 3TU, UK

<sup>b</sup> Department of Computer Studies, Loughborough University of Technology, Loughborough, Leics. LE11 3TU, UK

<sup>c</sup> Phase Separations Ltd., Deeside Industrial Park, Deeside, Clwyd CH5 2NU, UK

### Abstract

Gross flow development patterns have been monitored during slurry packing and compared for PEEK and stainless-steel liquid chromatographic microbore columns for different sorbents and slurry compositions. Flow-rate, pressure and apparent permeability data were collected with the help of a computer-aided monitoring technique. The development of the packing process under constant-pressure conditions, as detected by changes in the flow, has been found to have four characteristic stages, the development of which correlates with the final degree of compaction of the porous bed and with column efficiency. The parameters characterising porous structure – specific permeability,  $K_s$ , and specific column resistance,  $\phi'$  – have been compared for different groups of packed columns. It has been found that they correlate weakly with the column efficiency and the packing pressure for the same group of sorbents and packing slurry chemical composition. However, packings performed under the same pressure regime but using differing slurry media produced different flow patterns and have shown vast variation both in the column efficiency and in the specific column resistance. The range of specific column resistance values observed in this study for 0.5-mm I.D. microcolumns was  $250 < \phi' < 900$ . A correlation of  $\phi'$  with the column tubing material has been observed and attributed to wall effects.

The proposed method for the assessment of the effectiveness of the packing procedure enables changes in the dynamics of the packing process caused by changes of the slurry chemistry or other packing parameters to be observed and thus, the packing procedure for new stationary phases to be effectively adjusted. The expected column efficiency (and particularly packing failure) can be estimated during packing, prior to chromatographic assessment of the column.

**Keywords:** Slurry packing; Packing efficiency; Flow patterns; Stationary phases, LC

### 1. Introduction

The importance of the flow regime for efficient slurry packing has been widely discussed since the earliest publications on column packing [1–5]. Thus, Knox [1] stated that for analytical columns the regime of packing (constant pressure or constant

flow) is not of decisive importance, as long as a pressure gradient of 1000 bar/m or a flow-rate of 10 ml/min has been achieved. On the other hand, Andreolini et al. [2] suggested that “markedly different packing procedures are required for packing materials with different surface chemistry”. They observed that for cyano-bonded and unbonded silica gel a “slow” regime of packing was preferable, but for diol- and amino-modified silica gels “fast” regimes gave better results. Meyer and Hartwick [3] made a comparative study of the efficiency of the

\* Corresponding author. Present address: Institute of Analytical Instrumentation, Russian Academy of Sciences, Rizhskii pr. 26, St. Petersburg, 198103 Russian Federation.

flow and pressure regimes and recommended the use of a fixed pressure of around 12 000 p.s.i. (ca. 83 MPa) for the packing of microcolumns. They observed that loci of high efficiency correlated with column length at certain pressures. This observation suggests the existence of particular flow regimes favourable for packing. Karlsson and Novotny [4] described the packing of high-efficiency columns using a constant flow regime for columns with internal diameters in the range of 44–265  $\mu\text{m}$ . The efficiencies were inversely proportional to column diameter (note, however, that within this range of column diameters the initial drag force may differ by 36 times). High efficiencies for 0.32-mm I.D. columns were obtained by Bachman et al. [5] by using a constant pressure at 800 bar and a narrow 0.5-mm I.D. packing bomb. Other publications described constant pressure regimes for the packing of micro-bore and capillary columns, under pressures of 200–300 bar [6–9]. However, no studies have been reported so far on the relationship between the flow characteristics and the packing efficiency, even though the flow regime is closely connected with the velocity of the particles and the kinetic energy of their impact with the growing packed bed [10]. The control of the flow regime may be particularly important at moderate packing pressures, as used for the packing of polymer columns with a restricted strength limit [11,12].

The aim of the present work was to develop a method to monitor the gross flow during the slurry packing process and to investigate the correlation of the flow pattern with differing pressure regimes, packing and column materials and slurry compositions.

### 1.1. Theoretical background

As noted earlier [1] a sufficiently high impact velocity of particles into the packed bed is an important condition to produce a dense packing arrangement. This velocity depends on many factors of the flow, the most important of which for small particles are probably due to hydrodynamic, inertial and contact forces [12], whereas diffusion, gravity or pressure forces can be neglected. A particle in a

flowing fluid obtains velocity and acceleration in differing directions: rotational and translational. The component of the force parallel to the initial velocity of fluid is called a drag force,  $D$ . Under ideal conditions when the particles are smooth, the velocity profile of the fluid is flat, and the fluid is incompressible, then  $D$  is a function of the viscosity,  $\eta$ , density,  $\rho_f$ , and velocity of fluid,  $v$ , and particle diameter,  $d_p$  [12]. From dimensional analysis the following expression for the drag force was obtained [12]:

$$D = \frac{\pi}{8} d_p^2 \rho_f v^2 C_D(Re) \quad (1)$$

where  $C_D(Re)$  is the dimensionless empirical function of resistance, called drag coefficient, which depends on the Reynolds number,  $Re$  [13], where  $Re = \rho v d_p / \eta$  and  $v$  is the mean flow velocity. According to [12,13] the range of  $100 < Re < 500$ , which is characteristic for the initial stages of column packing, is within the so-called “intermediate range” where inertial forces are important and the flow becomes non-stationary. The flow around particles in this range does not follow the shape of the particle but produces individual eddies. The function  $C_D(Re)$  evaluated experimentally [12,13] together with Eq. 1 enables the drag force to be estimated for individual particles of a certain size.

With the growth of the column bed, the flow-rate,  $q$ , and the Reynolds number,  $Re$ , decrease. When the column is sufficiently filled the  $Re$  value falls below 1 and Darcy’s law (Eq. 2) is obeyed [14–16]:

$$q = - \frac{K_o P}{L \eta} \quad (2)$$

where  $K_o$  is the specific permeability,  $P$  is the pressure,  $L$  is the length of the column bed.  $K_o$  includes parameters associated with the porous structure of the bed, such as the interparticle porosity (ratio of void volume to total bed volume), surface roughness and bed packing geometry. Giddings [17] suggested that a more useful parameter than  $K_o$  for the analysis of porous packings in chromatographic applications is a flow resistance parameter,  $\phi'$ , which was later modified by Knox [18] and entitled

“specific column resistance”:

$$\phi' = \frac{Pd_p^2}{Lv\eta} \quad (3)$$

For sorbents with particle sizes of 5–10  $\mu\text{m}$  the range of  $\phi'$  was 600–700 [14]. A table of data for different columns was presented in a review by Knox [18].

## 2. Experimental

### 2.1. Chemicals

Tween 20 (polyoxyethylene-sorbitan monolaurate), ethylene glycol (spectroscopic grade), and sodium lauryl sulphate were obtained from Sigma (Poole, UK). Water, methanol, hexane, isopropanol, acetonitrile are all of HPLC grade (Fisons, Loughborough, UK).

### 2.2. Slurry preparation and packing materials

The slurries were prepared from the silica gels Spherisorb S5W (5  $\mu\text{m}$ , batch no. E05/135), Spherisorb S3W (3  $\mu\text{m}$ , batch no. 34/57), and Spherisorb S5 ODS2 (5  $\mu\text{m}$ , batch no. 34/14/1). Wide-pore Spherisorb S5X (5  $\mu\text{m}$ , batch no. SP3/145) was mixed with Spherisorb S5W batch no. D05121. All sorbents were obtained from Phase Separations (Deeside, UK). Silica gel slurries were dispersed in an aqueous 5% solution of Tween 20 diluted with ethylene glycol (1:1, v/v). The ODS-bonded silica gels were dispersed in 3% aqueous solution of sodium dodecyl sulphate with 1% sodium chloride. All slurries were subjected to sonification for 7 min before loading into the packing reservoir.

### 2.3. Packing equipment and procedure

The scheme of the experimental unit developed for the project and the outline of the slurry reservoir are presented in Fig. 1 (A and B, respectively). The column-packing unit consists of a slurry reservoir (1)

made of a stainless-steel tube 500 $\times$ 2 mm I.D. (part no. 55075, Phase Separations) attached to an ISCO 100D high-pressure syringe pump (ISCO, Lincoln, NE, USA) (5) through a stainless-steel tube of 250  $\mu\text{m}$  I.D. (part no. 550002, Phase Separations). The pump is connected to the computer (6) and plotter (7) for on-line data collection. A device for mechanical vibration of the column (4) with an amplitude of 2 mm and frequency around 25 Hz was installed perpendicular to its axis.

The pump was filled with eluent (methanol). Prior to packing, the slurry reservoir was loaded with slurry using the reverse movement of the pump piston at a flow-rate of 1.5 ml/min for 40–90 s (depending on the slurry concentration). After that the column (2) was attached to the lower end of the vertically positioned slurry reservoir (1) with a stainless-steel Parker-style end-fitting (part no. 613013, Phase Separations) (3) with a drilled funnel-like outlet (Fig. 1B). A constant pressure was applied abruptly and the parameters of the pump operation were collected as described below. The total packing time was 3 h.

### 2.4. Data collection

Flow and pressure data were collected from the ISCO pump controller through a RS-232-C serial interface by an Elonex PC-316X computer (Elonex, London, UK). The computer queried the pump once each second for the current values of flow-rate and pressure, recorded the data for later analysis and continually updated a graph of either flow-rate, pressure or the ratio of flow-rate to pressure versus time or logarithmic time. The graphical output may either be displayed on the computer's screen or plotted onto paper using a Roland DXY-880A plotter (Roland DG).

The accuracy of the regulation of the constant pressure by the pump controller as observed with the monitoring technique and an independent manometer was characterised by a standard deviation of less than 0.01% for the values measured once every second. The flow response was not as accurate and sometimes the pump had a tendency to produce microautooscillations. However, in most experiments

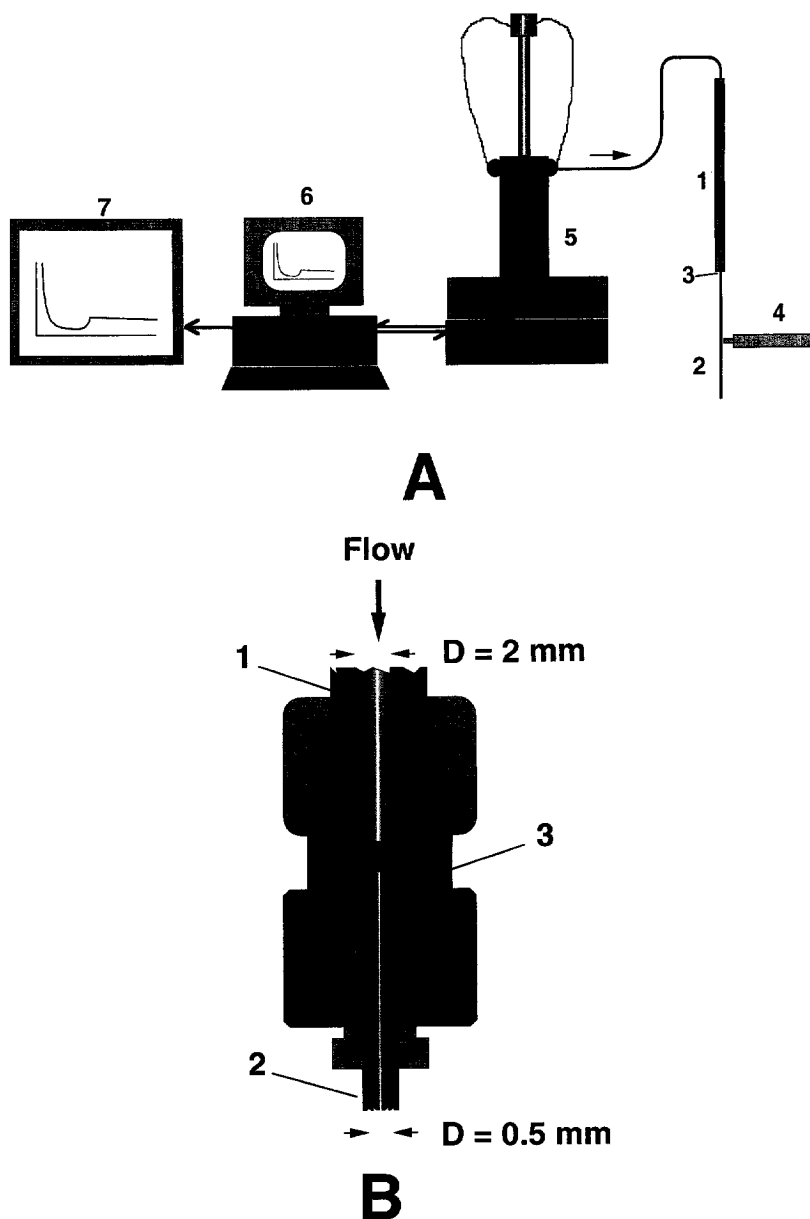


Fig. 1. Schematic representation of the laboratory unit for (A) the packing of microcolumns and (B) the outline of the packing bomb. 1=packing reservoir, 6.4×2 mm I.D.; 2=microbore column, 1.6×0.5 mm I.D.; 3=Parker-style 6.4×1.6 mm interface with funnel-like opening; 4=vibrator; 5=high-pressure syringe pump ISCO 100D; 6=computer; 7= plotter.

fluctuations of the flow-rate were random with a standard deviation of 0.1%. At the beginning of the packing process (10–14 s) a flow-rate spike was observed, which according to the pump manufacturer is due to a switch of regime of the pump.

### 2.5. Column preparation

PEEK columns were prepared from PEEK tubing of 1.6 mm O.D.×0.50 mm I.D. (part no. 560833, Phase Separations) cut to size with a home-made

guillotine. PEEK unions with two fingertight nuts and double ferrules Part 1061 (Jour Research, Onsala, Sweden) were used at the column outlet as end-fittings with 1.6-mm porous titanium frits with a mean pore size of 0.5 or 2  $\mu\text{m}$  (Valco Instruments, USA). The inlet of the column was fitted with a standard PEEK fingertight ferrule. Stainless-steel columns were prepared from stainless-steel tubing (316 grade, Part No. 550003), cut to lengths of 15, 25 or 30 cm (Phase Separations). Glass-lined steel columns of different standard lengths were also obtained from Phase Separations.

### 2.6. Column testing

For the column testing the outlets of the columns were fitted with PEEK unions as for packing containing 1-mm diameter titanium frits mounted in 1.6-mm PEEK rings obtained from Phase Separations. The top ends of the columns were installed directly into a Valco injector valve C14W with an internal volume of 60 nl (Valco) with the same type of titanium frits in PEEK rings as at the outlets of the columns.

The columns were tested using an HPLC system consisting of a PU 4010 reciprocating pump (Pye Unicam, Cambridge, UK) with a flow-rate range from 10  $\mu\text{l}/\text{min}$ , fitted with a home-made 1:4 flow-splitting system. The flow-rate was measured with a micro flow-meter (Phase Separations). The peaks were detected with an SSI variable UV-Vis 500 (Linear Instruments, Fremont, USA) fitted on-column with a capillary (75  $\mu\text{m}$ ) flow cell (Linear Instruments) with a virtual volume of 30 nl. The detection wavelength was usually 214 nm and the sensitivity range was 0.01–0.001 AU.

The columns packed with Spherisorb S5W were tested using cinnamyl alcohol with a binary eluent of isopropanol–hexane (4:96, v/v). The capacity factor was 2.0–2.5. The flow-rate was 2–10  $\mu\text{l}/\text{min}$ . The performance of the wide-pore Spherisorb S5X columns was measured using naphthalene ( $k=0$ ). The columns packed with Spherisorb S5 ODS2 were tested using fluorene ( $k=2$ –2.5) and a binary mixture of acetonitrile–water (70:30, v/v) as a mobile phase.

### 3. Results and discussion

The flow-rate,  $q$ , and pump pressure,  $P$ , values were monitored during the slurry packing for a number of PEEK, stainless-steel and glass-lined steel columns. Silica-gel-based stationary phases dispersed in differing media were used as the packing materials. The ratio of  $q$  and  $P$ , which may be defined as the apparent permeability,  $K_o^{\text{app}}$ , was also monitored as it is a useful parameter, independent of the pressure and according to Eq. 2 ( $q/P = -K_o/L\eta = K_o^{\text{app}}$ ) is proportional to the specific permeability,  $K_o$ .

Examples of the patterns of (gross) flow development versus time (for three packing pressures: 5000, 4000, and 3000 p.s.i., i.e. ca. 34, 28 and 21 MPa, respectively) recorded during the packing of Spherisorb S5W are presented in Fig. 2. The concentration of particles was 100 mg/ml in a viscous slurry medium consisting of an aqueous solution of Tween 20 and ethylene glycol. The choice of slurry medium and concentration was based on an earlier study in this laboratory of the packing of microbore columns [10]. Fig. 2A shows the flow-rate and Fig. 2B the corresponding  $K_o^{\text{app}}$  values recorded for the packing of PEEK columns (length 35 cm  $\times$  0.5 mm I.D.). (The nominal applied pressure was used for the calculation of  $K_o^{\text{app}}$ , as the flow resistance of the porous titanium frits is estimated as practically equal to zero and was neglected.) The curves from replicate packings corresponded closely. An analysis of the data from a large number of packings has shown that the development of the flow for the above system may be divided into four stages as described below.

The first stage (I in Fig. 2A), which lasts several seconds, is characterised by high Reynolds numbers ( $Re=400$ –500) as the linear flow velocity is around 2 m/s. This initial stage of the process may not be stable and reproducible in terms of the local flow. These  $Re$  values are classified elsewhere as “intermediate” range [12,13], which is characterised by the formation of detached vortices, an instability of flow due to the oscillation of vortices and an increase in the influence of inertial forces on the movement of particles which altogether reduce the drag force [13]. However, due to the high mean linear velocity of the liquid front and a second-order dependence of  $D$  on

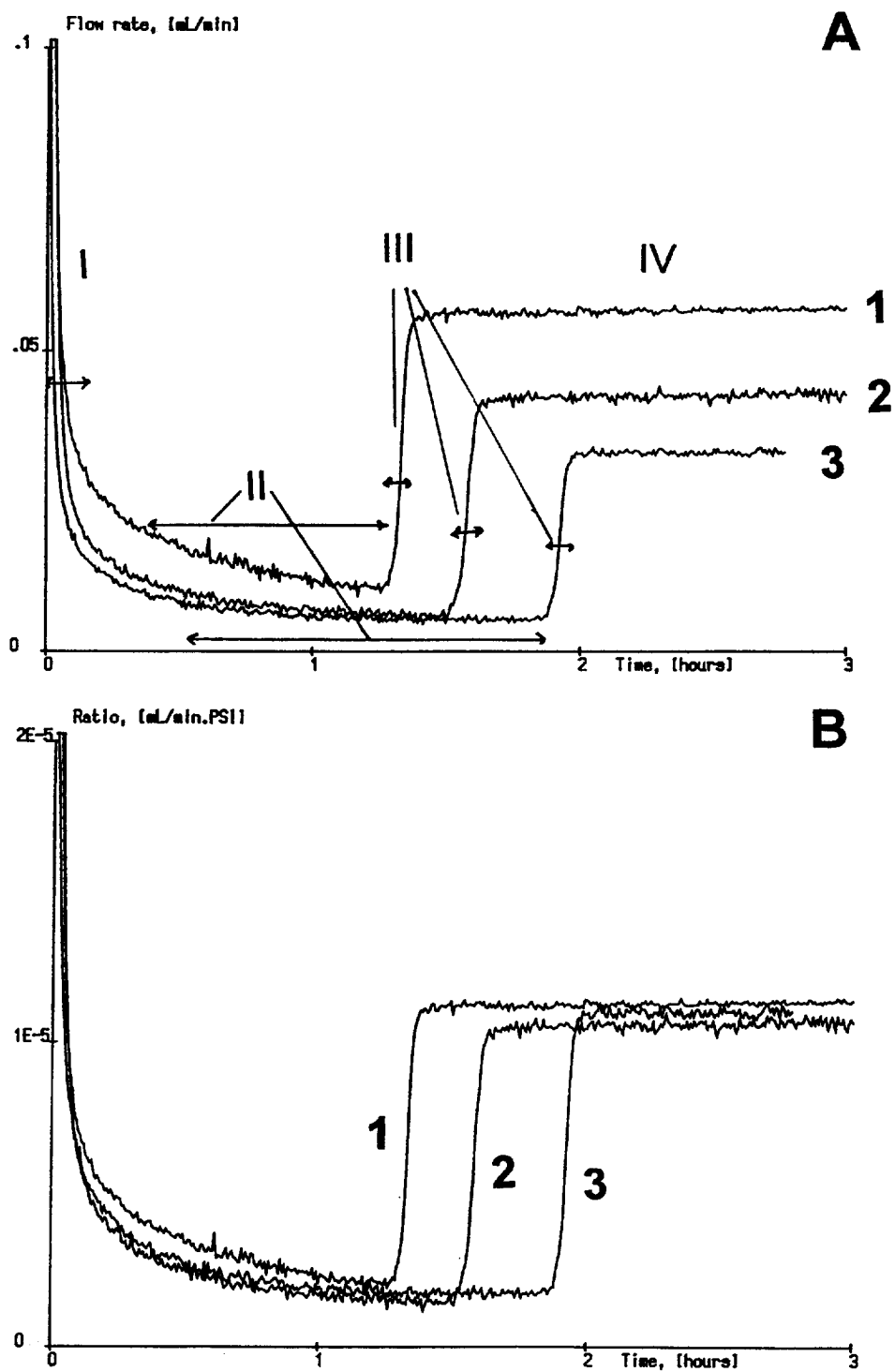


Fig. 2. Flow patterns recorded during the packing of Spherisorb S5W into PEEK column, 350×0.5 mm I.D. at three different pressures: 1=5000 p.s.i., ca. 34 MPa; 2=4000 p.s.i., ca. 28 MPa; 3=3000 p.s.i., ca. 21 MPa. For definition of ranges I–IV see text. (A) Flow-rate; (B) apparent specific permeability,  $K_o^{app}$ .

$q$  (Eq. 1) the overall drag force probably grows with increasing the flow-rate. Thus, at the beginning of the packing process, when flow-rate is at a maximum (25 ml/min), the drag force acting on the silica gel particle of  $d_p=5$  mm dispersed in a viscous aqueous solution of Tween 20 ( $\rho=1.03$  ml/g) can be estimated with the help of Eq. 1 and coefficient  $C_D(Re)=1$  [13] as approximately  $4 \cdot 10^{-8}$  N. In contrast, near the Darcy region (typical for a constant flow regime) with a flow-rate of 0.1 ml/min and  $C_D(Re)=300$  [13] the drag force would be  $2 \cdot 10^{-10}$  N. Thus, a constant pressure regime, in comparison with constant flow conditions gives an initial drag force two orders of magnitude higher. During this stage an immature loose porous bed is being rapidly formed in the column volume. Formation of this porous bed makes it possible to start assessment of the  $K_o^{app}$  of the packing bed, as this reflects the progress of the compaction process. During the initial 10–12 s of the packing the flow-rate falls from 25 ml/min to 0.1 ml/min.

The second stage (II in Fig. 2) can be characterised by the values of Reynolds number within the range  $0.1 < Re < 1$ . During this stage the packed bed gradually undergoes further compaction under the influence of the drag force produced by the viscous slurry media and agitation by vibration. The duration of the compaction stage depends on the viscosity of the slurry media, the volume of the slurry, which had been loaded into the reservoir, and the flow-rate. At the end of this period, if the compaction is successful, a minimum flow-rate, sometimes as low as 1–5  $\mu$ l/min is usually reached.

This is followed by the third stage (III in Fig. 2) when the front of the conditioning eluent, methanol in this study, migrates through the column. Due to the lower viscosity of the conditioning eluent the flow-rate increases, producing a step on the flow pattern. This stage may increase the stability of the positions of the particles within their three-dimensional arrangement due to the changes in the local velocity.

Finally the bed undergoes an equilibrating stage under the influence of the less viscous eluent flowing with a higher linear velocity (stage IV in Fig. 2). At this stage the Reynolds number is approximately within the same range ( $Re=0.5-1$ ). If the packing arrangement is dense and stable, the flow-rate during

this stage is constant. However, if the packing is loose, then further compaction may be observed, manifesting itself as a gradual decrease in the flow-rate.

The development of each stage, particularly the first and second, is important as they define the final geometry of the packing. During the total course of packing under the constant pressure conditions, the flow regime changes over a wide range, characterised by the three orders of magnitude change in the Reynolds number ( $0.1 < Re < 400$ ).

Data for the same slurry compositions and slurry volumes but obtained with different applied pressures have similar profiles (Fig. 2). At higher pressures the overall flow-rates increase and the resulting column efficiency improves. In each case the high flow-rate (stage I) regime takes a few minutes. The next stage (II) depends upon the pressure conditions and finishes within 0.5–2 h (for the moderately viscous media of 2–5 stokes, using surfactants). The front of the eluent (methanol) produces a sharp step (stage III) which occurs earlier at higher pressures because of the higher flow-rates. The conditioning plateau (stage IV) is characterised by a constant flow-rate showing that the packing arrangement is stable. The columns from this group proved to have good performances. The specific column resistance of a number of columns packed under these conditions over a range of pressures correlates with the pressure used for packing (Fig. 3A) and resulting column efficiency (Fig. 3B). However, both correlations are weak. The specific column resistances differed over only a small range although the reproducibility of the values for replicate columns packed under the same applied pressure conditions was good (Fig. 3A).

The pressurisation of the whole packing system including the pump volume of 100 ml takes a relatively short time, approximately 3–5 s, due to the design of the ISCO pump with two regimes of the motor. However, it is necessary to consider the compression of the eluent in the relatively large pump volume, 100 ml. In Fig. 4 the flow patterns for the packing of Spherisorb S5W under the pressure of 5000 p.s.i. (ca. 34 MPa) into the PEEK column (A) and pressurisation of the pump with a closed outlet valve at the same pressure (B) are presented. The subtraction of the curve B from curve A would give

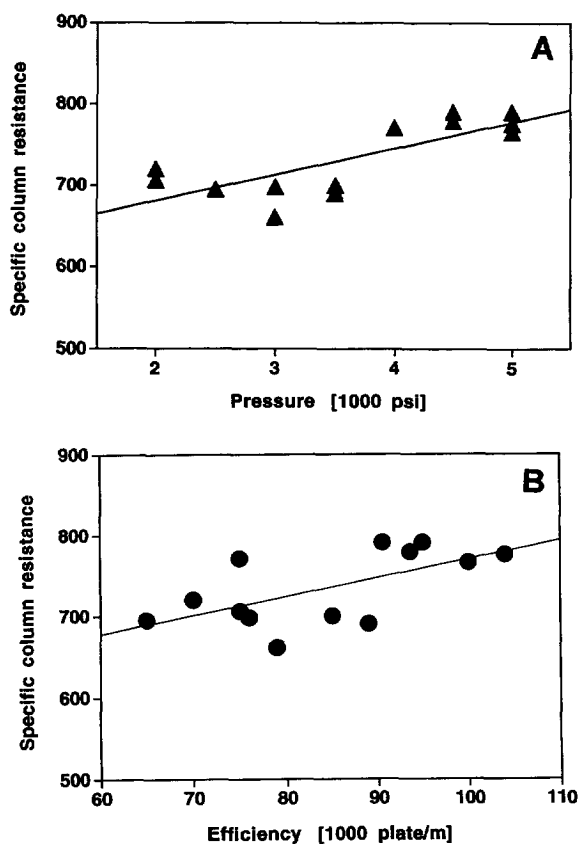


Fig. 3. The relationship of (A) the specific permeability versus packing pressure and (B) specific column resistance versus column performance for a sample of PEEK columns (0.5 mm I.D.) columns packed with Spherisorb S5W dispersed in aqueous Tween 20/ethylene glycol under differing packing pressures.

a more accurate flow profile. The spikes in the flow curve output were reproducible and were thought to result from an effect of the pump design when it changes from a high unrestricted initial movement of the pump head to a region which is controlled by the constant pressure feedback.

Variation of the packing parameters has shown that the characteristic flow pattern during packing under constant pressure, is determined to a large extent by the nature of the sorbent and composition of the slurry. In Fig. 5 two groups of flow patterns obtained for silica gels packed into PEEK micro-columns of 0.5 mm I.D. are shown. The first group

(Fig. 5A) represents the packing process of wide-pore Spherisorb S5X (curve 1) and its mixtures with Spherisorb S5W, 1:1, w/w (2) and 1:2, w/w (3), respectively. The corresponding curve for Spherisorb S5W alone was shown earlier in Fig. 2 (curve 1). The concentration of the slurries dispersed in aqueous solution of Tween 20 with ethylene glycol was 100 mg/ml, and the applied pressure was 5000 p.s.i. (ca. 34 MPa) in all cases. Under the same pressure regime the flow patterns show different durations of the stages and finally different column efficiency. Thus, in the case of a wide-pore silica gel (curve 1), stage I is very short and formation of the primary column bed is completed very quickly. The compaction stage (II) is rather short as well; however, it has almost no slope showing that the bed is already dense. The resulting column is well packed, with efficiency obtained for naphthalene ( $k=0$ ): 60 000 plates/m. The addition of 50% (w/w) of narrow-pore Spherisorb S5W (curve 2) increases the duration of stage I, which could be due to the inhomogeneity of the density of the particles and surface texture in the slurry leading to the increase of turbulence and finally to a reduction in the average drag force. The resulting column efficiency is lower (45 000 plates/m). A further increase in the proportion of the narrow-pore silica gel fraction (67%, v/v, curve 3) produces an increased duration of the stage II, due to the higher flow resistance of narrow-pore silica gel. The resulting column efficiency is 31 000 plates/m (for naphthalene). Finally, as discussed earlier the curve for Spherisorb S5W alone showed a steep initial curve with a fairly flat plateau and a longer stage II indicating a high specific resistance.

The second group of data (Fig. 5B) demonstrates the flow patterns during the packing of wide-pore Spherisorb S5X using the same applied pressure but differing slurry media. Thus, curve 1 is the same as in Fig. 5A, whereas curves 4 and 5 are the patterns for slurries dispersed in aqueous HCl solution at pH 2 and in water, respectively, and curve 6 is for a slurry dispersed in methanol–water (50:50, v/v). The different slurry media demonstrated significant flow pattern variations as well as changes in the resulting column efficiency. The three curves (4, 5 and 6) reflect particles packed into loose beds with a low specific column resistance. Curve 5 (for a slurry



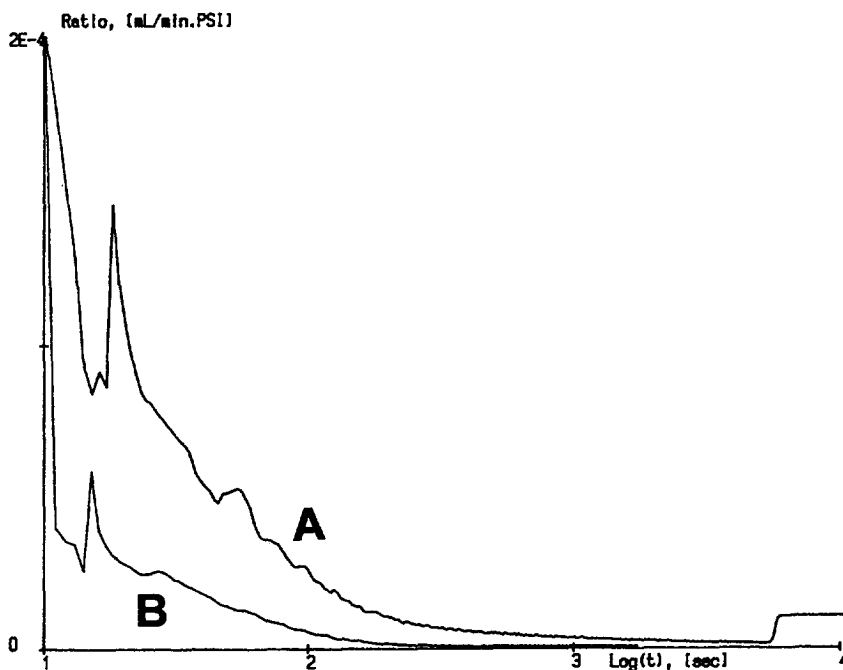


Fig. 4. Flow patterns recorded (A) for the packing of Spherisorb S5W into PEEK 350×0.5 mm I.D. at 5000 p.s.i. (ca. 34 MPa) and (B) for pressurisation of the pump at the same pressure with closed outlet valve.

dispersed in water, when silica gel particles are charged) shows the compaction of the packed bed during the conditioning phase (stage IV), confirming its unstable loose packing arrangement. Although, a similar pattern was not observed for the slurry dispersed in a solution of HCl (curve 4) or for the slurry in methanol–water (curve 6), where the silica gel particles are electrically neutral, the packing in these cases was also poor, as these media do not produce the optimal hydrodynamic conditions for obtaining high drag force [10]. The efficiencies of columns as measured by naphthalene for cases 4–6 (Fig. 5) were 10 000–20 000 plates/m. The efficiency and specific column resistance values calculated according to Eq. 3 using the values of  $K_0^{app}$  from the flow graphs for this group of columns are presented in Table 1.

Another example of the influence of the slurry media on the flow pattern and on the final column efficiency is presented in Fig. 5C. PEEK columns were packed with Spherisorb S5 ODS2 dispersed in

SDS solution (curve 7) and in Tween 20 (as for normal-phase silica gel) (curve 8). Curve 7 shows a rapid reduction in the flow-rate in stage I and a horizontal plateau in stage II, and gave a good column efficiency of 85 000 plates/m. Flow pattern 8 recorded for the non-homogeneous slurry (see Ref. [10]) shows the continuous compression of agglomerates during stage II and gave rather poor efficiency, 40 000 plates/m even though the final flow-rate is similar.

Thus, when the duration of stage I is short, i.e. the initial bed is formed quickly, the columns are better packed. Stage II should have sufficient duration to compress the bed, and the presence of a plateau with a low negative or negligible slope indicates that packing is progressing well. A more detailed graph of the progress of the initial stages of the packing can be obtained by reexamining the curves from Fig. 5 using a logarithmic time scale (Fig. 6). The records of  $K_0^{app}$  against  $\log t$  for three of the columns demonstrate that for a “good” column (curve 1) the

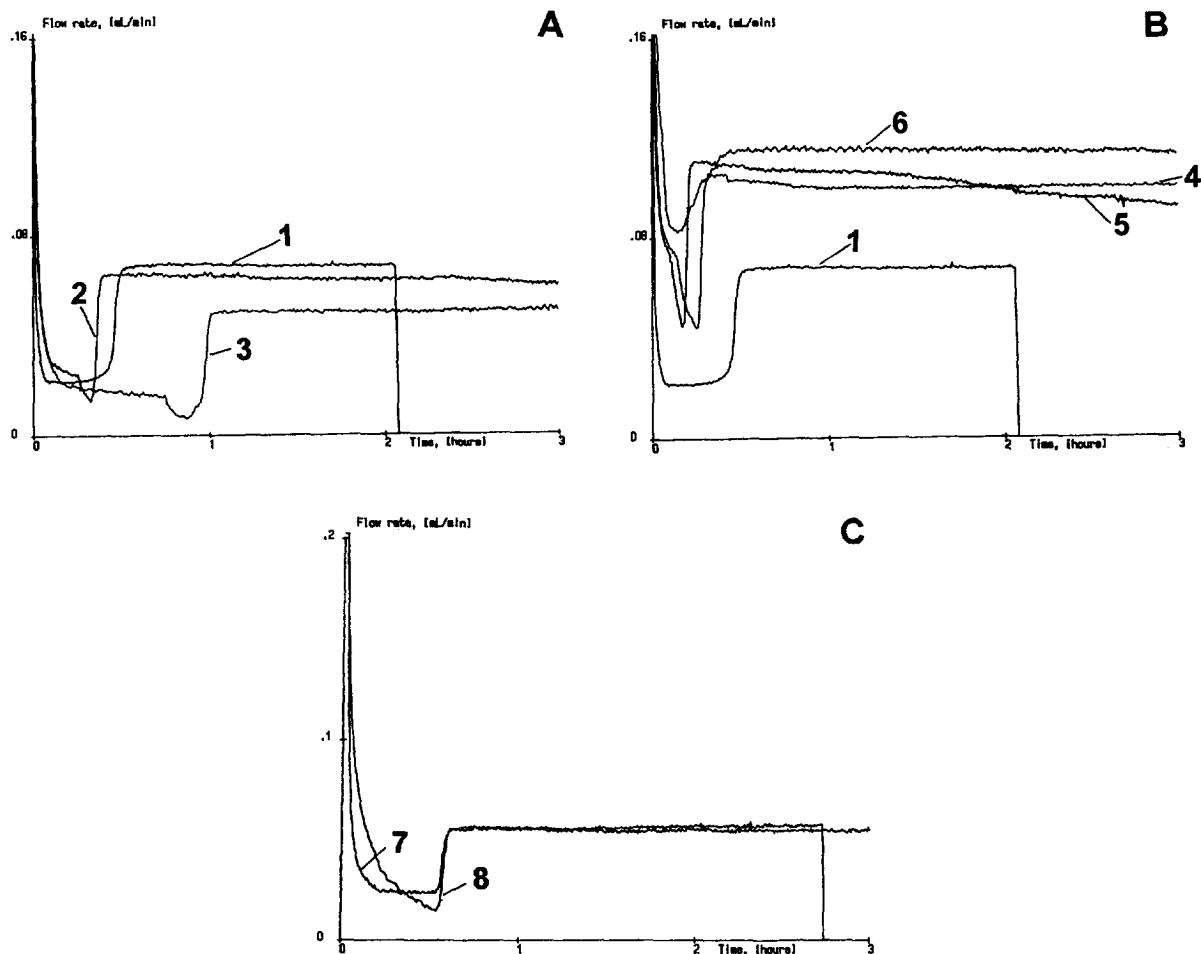


Fig. 5. Flow-rates versus time recorded for groups of PEEK columns. Pressure 5000 p.s.i. (ca. 34 MPa) in all cases. (A) The influence of the composition of the sorbent with a slurry medium of aqueous Tween 20/ethylene glycol. Sorbent composition: 1=Spherisorb S5X; 2=Spherisorb S5X/S5W (1:1, w/w); 3=Spherisorb S5X/S5W (1:2, w/w). (B) The influence of the slurry media on the flow pattern for the packing of Spherisorb S5X. Slurry media curves: 1=same as in (A); 4=aqueous solution of HCl, pH 2; 5= water; 6=water-methanol (50:50, v/v). (C) The effect on bonded phases. Packing of Spherisorb S5 ODS2. Slurry media curves: 7=aqueous SDS with NaCl; 8=Tween 20/ethylene glycol.

Table 1

Specific column resistance,  $\phi'$  and efficiency,  $N$  (at  $k=0$ ), for PEEK columns packed with mixtures of Spherisorb S5W and wide-pore Spherisorb S5X in differing blends and slurry compositions (as given in Fig. 5)

Sorbent	Slurry media	$N$ (plates/m)	$\phi'$
Spherisorb S5X	Tween 20, water/ethylene glycol	60 000	414
Blend: S5X/S5W (1:1, w/w)	Tween 20, water/ethylene glycol	37 000	553
Blend: S5X/S5W (1:2, w/w)	Tween 20, water/ethylene glycol	29 000	462
Spherisorb S5X	Water	12 000	245
Spherisorb S5X	Aqueous HCl, pH 2	10 000	304
Spherisorb S5X	Water-methanol (1:1, v/v)	14 000	276

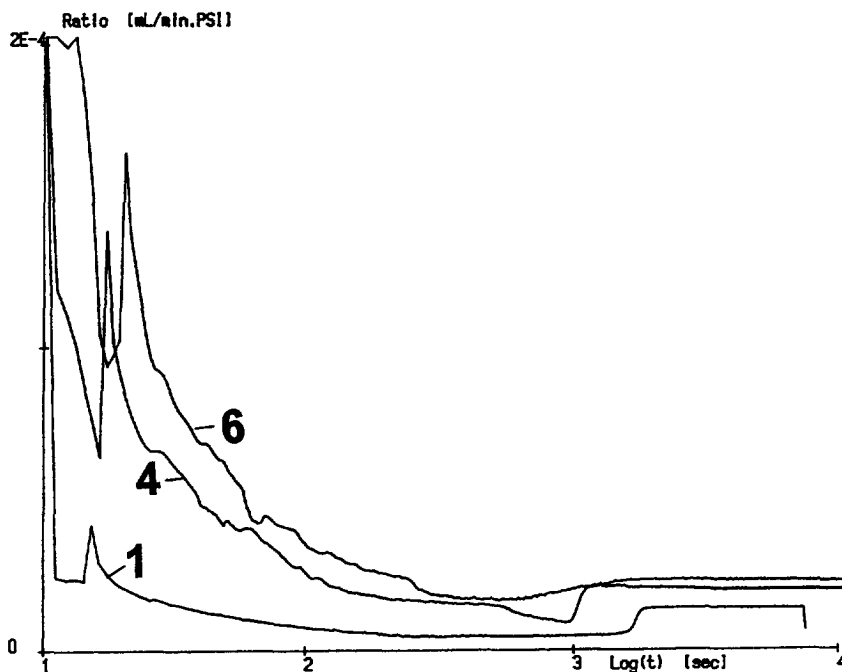


Fig. 6. Expanded logarithmic time scale for the early part of the packing process. Columns numbered as in Fig. 5. Plot of apparent specific permeability,  $K_o^{app}$  versus  $\log t$ .

initial period of packing is short whereas for curve 4 (dilute HCl slurry) and curve 6 (methanol–water slurry) the initial stages are more prolonged.

The analysis of column performance, and its correlation with packing conditions, enables us to conclude that the chemical composition of the slurry medium is the most important criterion for obtaining well-packed columns and this confirms our earlier study of packing microbore columns [10]. Thus, the columns from Table 1, packed with blends of sorbents with different pore sizes and using different slurry media but an identical packing regime have produced a vast variation of column efficiency ( $10\,000 < N < 60\,000$ ) and specific column resistance ( $245 < \phi' < 553$ ). However, a sample of columns packed using identical slurry composition but different packing pressures within the range 2000–5000 p.s.i. (250%) (ca. 14 to 34 MPa) had a standard deviation for the efficiency of only 14% and for the specific column resistance of only 6%. Thus, the pressure conditions, although important, do not

negate the importance of the selection of an appropriate chemical composition for the slurry medium.

Qualitatively similar data were obtained for packing into stainless-steel and glass-lined steel columns. Values of  $\phi'$  have been estimated on the basis of the  $K_o^{app}$  obtained during the packing of a number of columns prepared from different column materials (Fig. 7). As expected the specific column resistance proved to be higher for columns packed with narrow-pore particles, Spherisorb S5W and S5 ODS2, than for wide pore, Spherisorb S5X. However, the same type of sorbent packed into PEEK tubing gave columns with a lower specific permeability than stainless-steel columns and glass-lined steel columns (though the latter were packed at a higher pressure of 10 000 p.s.i.; ca. 69 MPa). This can be explained by a lower local porosity along the walls of PEEK tubing due to the irregular structure of the surface. This assumption has been studied further with the help of scanning electron microscopy. The internal surfaces of PEEK tubing previously used for packing

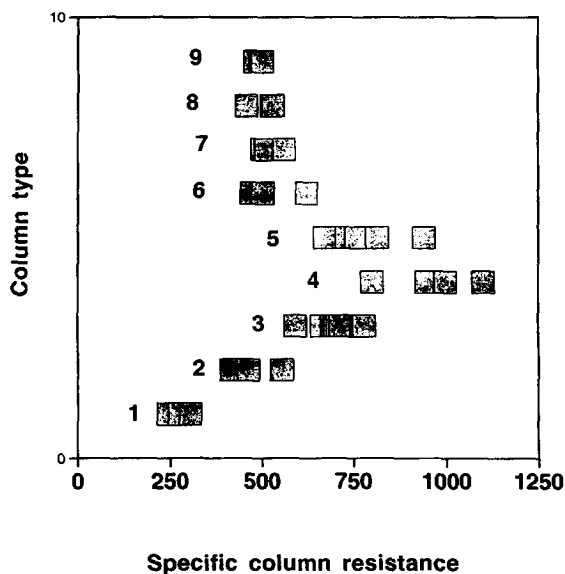


Fig. 7. Specific column resistances for groups of columns packed with different stationary phases using different column materials: 1=loosely packed wide-pore Spherisorb S5X in PEEK column; 2=same as 1 but densely packed; 3=Spherisorb S5W in PEEK column; 4=Spherisorb S3W in PEEK column; 5=Spherisorb S5 ODS2 in PEEK column; 6=Spherisorb S3W in stainless steel; 7=Spherisorb S5 ODS2 in stainless steel; 8=Spherisorb S5 ODS2 in glass-lined steel; 9=Spherisorb S5W in stainless steel.

were observed at different magnifications. The internal surface of PEEK tubing has a dimpled texture with sub-micrometer features, which can accommodate particles in the recesses and thus reduce local porosity. However, no evidence of the silica gel particles being embedded into the walls of the PEEK columns has been found.

#### 4. Conclusions

Real-time monitoring of the column-packing procedure enables observation of changes in the gross flow caused by the variation of chemical composition of the slurry, or of packing pressure, which can be correlated with the resulting column performance. The monitoring enabled the packing quality to be assessed during the packing process and prior to chromatographic testing. It is particularly useful for observing packing failure. The analysis of apparent specific column permeability,  $K_o^{app}$ , and specific

column resistance,  $\phi'$ , data obtained with the help of this method for a large number of columns has shown that these characteristics of the porous media correlate with the efficiency of the columns and the packing pressure, but that the correlation is weak. However, both of these parameters strongly depend on the chemical composition of the slurry, which also affects the flow development pattern. The characteristic ranges of the specific column resistance for microbore columns were as follows: PEEK, Spherisorb S5 ODS2,  $600 < \phi' < 900$ ; PEEK, Spherisorb S5,  $680 < \phi' < 800$ ; PEEK, wide-pore Spherisorb S5X,  $400 < \phi' < 550$  and for stainless-steel columns around 500.

#### Acknowledgments

The authors wish to thank DTI and SERC (now EPSRC) for their support of this work within the TAPM-LINK project "Microbore columns for liquid chromatography". Dr. M.C. Ball at Loughborough University is acknowledged with thanks for his help with electron microscopy.

#### References

- [1] J.H. Knox (Editor), High-Performance Liquid Chromatography, Edinburgh University Press, Edinburgh, 1978, pp. 147–156.
- [2] F. Andreolini, C. Borra and M. Novotny, *Anal. Chem.*, 59 (1987) 2428.
- [3] R.F. Meyer and R.A. Hartwick, *Anal. Chem.*, 56 (1984) 2211.
- [4] K.-E. Karlsson and M. Novotny, *Anal. Chem.*, 60 (1988) 1662.
- [5] K. Bachmann, I. Haag and T. Prokop, *Fresenius J. Anal. Chem.*, 345 (1993) 545.
- [6] R. Gill, *J. Chromatogr.*, 354 (1986) 169.
- [7] R.T. Kennedy and J.W. Jorgenson, *J. Microcol. Sep.*, 2 (1990) 120.
- [8] S. Hoffmann and L. Blomberg, *Chromatographia*, 24 (1987) 416.
- [9] C. Yan, D. Schaufelberger and F. Erni, *J. Chromatogr. A*, 670 (1994) 15.
- [10] T.M. Zimina, R.M. Smith, P. Myers, B.W. King, *Chromatographia*, 40 (1995) 662.
- [11] T.M. Zimina, R.M. Smith, P. Myers and B.W. King, *Chromatogr. Anal.*, 37 (1995) 5.

- [12] R.H. German, Particle Packing Characteristics, MPIF, Princeton, NJ, 1989.
- [13] H. Schlichting, Boundary Layer Theory, 4th ed., Verlag G. Braun, Karlsruhe, 1960, p. 16.
- [14] L. Streeter, Fluid Mechanics, McGraw-Hill, New York, 1966, p. 251.
- [15] A. Dybbs and R.V. Edwards, in J. Bear and M.Y. Corapcioglu (Editors), Fundamentals of Transport Phenomena in Porous Media, 1984, NATO ASI Series, Vol. 82, p. 199.
- [16] A.L. Dullein, Porous Media Fluid Transport and Pore Structure, Academic, New York, 1979.
- [17] J.C. Giddings, Dynamics of Chromatography. Part 1, Marcel Dekker, New York, 1965, p. 195.
- [18] J.H. Knox, in C.F. Simpson (Editor), Techniques in Liquid Chromatography, Wiley, Chichester, 1982, p. 31.